H5EPTPACH2OH: Synthesis, Relaxometric Characterization and 1H NMR Spectroscopic Studies on the Solution Dynamics of Its LnIII Complexes

Susana Torres,[a] José A. Martins,*[a] João P. André,*[a] Giovannia A. Pereira,[b] Robert Kiraly,[c] Ernö Brücher,[c] Lothar Helm,[d] Éva Tóth,[e] and Carlos F. G. C. Geraldes*[b]

The synthesis and characterization of a new metal chelator, 4-(S)-hydroxymethyl-3,6,10-tri(carboxymethyl)-3,6,10-triaza-dodecanedioic acid (H5EPTPACH2OH), is reported. Protonation constants for the ligand H5EPTPACH2OH and for the previously reported H5EPTPAC16 have been determined by potentiometry, which reveals that both ligands display slightly higher protonation constants relative to that of the ligand DTPA^{5-}. The stability constant for the [Gd(EPTPA-CH2OH)(H2O)]$^{2-}$ complex has also been determined by potentiometry. The obtained value (log K_{GdL} = 16.7) is two orders of magnitude lower than that for the [Gd(EPTPA)-(H2O)]$^{2-}$ complex, which indicates the destabilizing effect of the pendant hydroxymethyl group at the EPTPA backbone. The microscopic protonation scheme has been deduced from the pH dependence of the 1H NMR spectra of both H5EPTPACH2OH and H5EPTPAC16 ligands. The first two protonations occur exclusively at the backbone nitrogen atoms – the first protonation occurs preferentially at the more

basic central nitrogen atom. The second proton distributes preferentially between the two terminal nitrogen atoms with the favoring of the trimethylene nitrogen atom over the ethylene nitrogen atom. The LnIII complexes of the ligand H5EPTPACH2OH have been prepared and their solution dynamics studied by 1H NMR spectroscopy. Two sets of resonances of very different intensities from two isomeric complexes have been observed. Relaxometric investigations (17O NMR and 1H NMRD) demonstrate that the [Gd(EPTPA-CH2OH)(H2O)]$^{2-}$ complex displays an accelerated water-exchange rate (k_{ex} = 87.6 × 10^6 s^{-1}) that is close to the theoretically derived optimal value. However, the kinetic stability of this complex in phosphate-buffered solutions towards Zn^{2+} transmetallation is quite low, but higher than that of the corresponding methyl derivative.

(© Wiley-VCH Verlag GmbH & Co. KGaA, 69451 Weinheim, Germany, 2007)

Introduction

Magnetic resonance imaging (MRI) uses radiofrequency waves and a strong magnetic field to provide remarkably clear and detailed pictures of internal organs and tissues. The development of this imaging modality parallels the emergence of a new class of metallopharmaceutics, known as contrast agents (CAs).[1,2] Contrast agents are primarily GdIII complexes because this metal ion has seven unpaired electrons and a slow electronic relaxation rate.[3]

In fact, the image-enhancing capability of the commercially available poly(aminocarboxylate)-based chelates is only a few percent of the maximum value predicted by the Solomon–Bloembergen–Morgan theory.[4,5] In order to attain maximum relaxivities, the rotational correlation time (τ_r), proton-exchange rate (k_{ex}), and electronic spin relaxation rates (T_e) have to be optimized simultaneously.[4,5]

The covalent attachment of GdIII chelates to slow-tumbling macromolecules (linear polymers,[6] carbohydrates,[7] proteins,[8] and dendrimers[9]) and the formation of host–guest noncovalent interactions between GdIII chelates and macromolecules[10] are successful strategies to increase τ_r. An alternative way to achieve this goal is through self-assembly of amphiphilic GdIII chelates[11] or through the inclusion of lipophilic GdIII chelates in liposomes[12] or other lipid-based colloidal systems.[13]

In spite of the efforts to optimize the rotational correlation time of slow-tumbling GdIII complexes, the relaxivity

[a] Centro de Química, Campus de Gualtar, Universidade do Minho,
4710-057 Braga, Portugal
Fax: +351-253-678-983
E-mail: jmartins@quimica.uminho.pt
jandre@quimica.uminho.pt
[b] Departamento de Bioquímica, Faculdade de Ciências e Tecnologia, Universidade de Coimbra, Apartado 3126,
3001-401 Coimbra, Portugal
Fax: +351-239-853-607
E-mail: geraldes@ci.uc.pt
[c] Department of Inorganic and Analytical Chemistry, University of Debrecen,
4010 Debrecen, Hungary
[d] Laboratoire de Chimie Inorganique et Bioinorganique, Ecole Polytechnique Fédérale de Lausanne, EPFL-BCH,
1015 Lausanne, Switzerland
[e] Centre de Biophysique Moléculaire, CNRS,
Rue Charles Sadron, 45071 Orléans, France
▢ Supporting information for this article is available on the WWW under http://www.eurjic.org or from the author.

enhancement achieved may be limited if the water-exchange rate (k_{ex}) is not simultaneously optimized. When the water-exchange rate is too fast, the protons are not effectively relaxed. Conversely, the coordination site is needlessly occupied by a relaxed water molecule. Most Gd[III] complexes investigated to date as potential contrast agents have very slow water-exchange rates ($k_{ex} \approx 10^6$ s^{-1}), far from its optimal value (about $k_{ex} = 10^8$ s^{-1}).

The water exchange in Gd[III] complexes is essentially determined by two factors, both of which can, to some extent, be controlled by design.[14] The first and most easily controlled factor is the electron density on the central lanthanide ion. Electron deficiency on the metal ion results in slow dissociation of the bound water molecule as a result of the enhanced electrostatic attraction responsible for the shortening of the lanthanide–water bond. Therefore, ligands containing anionic groups (e.g. carboxylates) are responsible for a fast water exchange, whereas neutral ligands (e.g. amides or alcohols) would favor slower water exchange. Another way of obtaining Gd[III] complexes with fast water exchange rates is related to the design of ligands that display an increased steric hindrance around the water coordination site. Muller and co-workers have reported a reduction in the time of residence of the bound water molecule (τ_M; $\tau_M = 1/k_{ex}$) for a series of Gd[III]–DTPA complexes bearing diverse substituents on the C4 carbon atom of the ethylene bridge: Gd(S)-C4-Me-DTPA ($\tau_M^{310} = 91$ ns), Gd(S)-C4-nBu-DTPA ($\tau_M^{310} = 82$ ns), Gd(S)-C4-iBu-DTPA ($\tau_M^{310} = 108$ ns), Gd(S)-C4-iPr-DTPA ($\tau_M^{310} = 98$ ns), and Gd-C4-diMe-DTPA ($\tau_M^{310} = 57$ ns) relative to that of the parent Gd[III]–DTPA complex ($\tau_M^{310} = 143$ ns).[15] The same effect has been reported by the same authors for Gd[III]–DTPA complexes bearing ethoxybenzyl,[16] benzyl,[17] and (4,4-diphenylcyclohexyl)phosphonooxymethyl[18] substituents on the C4 carbon atom of the ethylene bridge. A comparative study of the four possible regioisommerically benzyl-functionalized Gd[III]–DTPA complexes showed that substitution at C4 (next to the ethylene bridge terminal nitrogen atom) and C7 (central acetate) yields higher steric hindrance of the coordinated water molecule (with a corresponding higher increase in the water-exchange rate) than substitution at C5 (next to the ethylene bridge central nitrogen atom) and C2 (terminal acetate).[19] However, substitution at C5 and C4 are the most effective in sterically reducing the accessibility of Zn^{2+} to the ligand, and thus are the most protective against transmetallation by this ion.[19]

Merbach et al. also demonstrated that the insertion of an extra methylene group to the backbone or to a pendant arm in macrocyclic tetraacetate complexes and to DTPA-derived complexes causes steric compression around the water-binding site, with a corresponding increase in the bound-water-exchange rate (k_{ex}) by a factor of one or two orders of magnitude for [Gd(DTTA-prop)(H$_2$O)]$^{2-}$ and [Gd(EPTPA-bz-NO$_2$)(H$_2$O)]$^{2-}$, respectively.[20] In solution, lanthanide(III) complexes of H$_4$DOTA-like ligands are typically present as a mixture of two diastereoisomers: the square antiprismatic (SAP) or M ("major") and the twisted square-antiprismatic (TSAP) or m ("minor") isomer.[21] Studies revealed that these isomers display different τ_M values.[22] The neighborhood of the water molecule in a TSAP isomer is more sterically crowded, and therefore the water molecule exchanges 10–100 times faster than in a SAP isomer. Therefore, Gd[III] complexes displaying, in solution, exclusively the TSAP isomer could potentially lead to high relaxivity CAs.

In this paper, we report the synthesis and characterization of the ligand 4-(S)-hydroxymethyl-3,6,10-tris(carboxymethyl)-3,6,10-triazadodecanedioic acid (**1**, H$_5$EPTPA-CH$_2$OH) and of its Ln[III] complexes and compare the properties of this ligand with that of its hexadecanoyl ester derivative (**2**, H$_5$EPTPAC16)[23] [Figure 1]. The protonation constants were determined for both ligands by potentiometry, and their microscopic protonation scheme was obtained with NMR pH titrations. For ligand **1**, the stability constant of the Gd[III] complex was also obtained by potentiometry, and the solution dynamics of several Ln[III] complexes was studied by ^{1}H NMR spectroscopy. ^{17}O NMR and NMRD measurements have been performed on the [Gd(EPTPACH$_2$OH)(H$_2$O)]$^{2-}$ complex, thus allowing us to determine the parameters that govern its relaxivity. Its stability towards Zn^{2+} transmetallation was also tested.
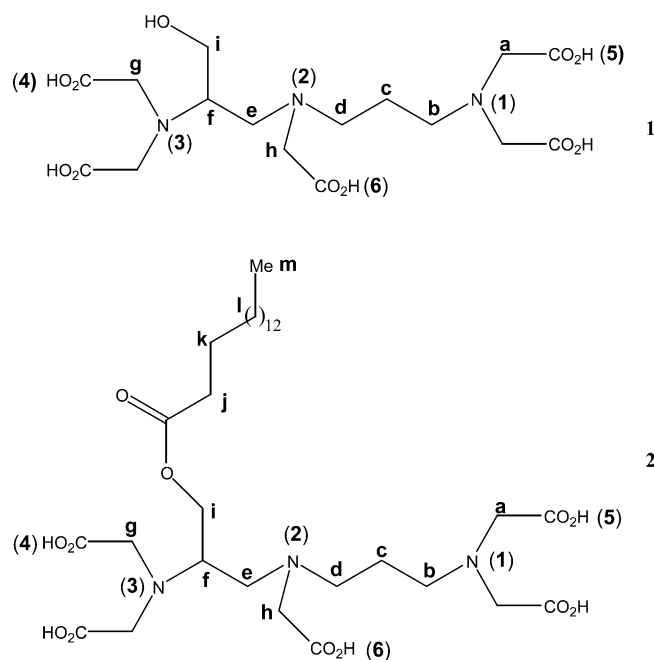

Figure 1. Chemical structures of the ligands H$_5$EPTPACH$_2$OH (**1**) and H$_5$EPTPAC16 (**2**). Arbitrary numbers and labelling is shown for convenience of the ^{1}H NMR assignment.

Results and Discussion

Synthesis of the Ligands

We have recently reported a new synthetic path to metal chelators based on the EPTPA skeleton bearing a hydroxymethyl group on the ethylenediamine unit. The substi-
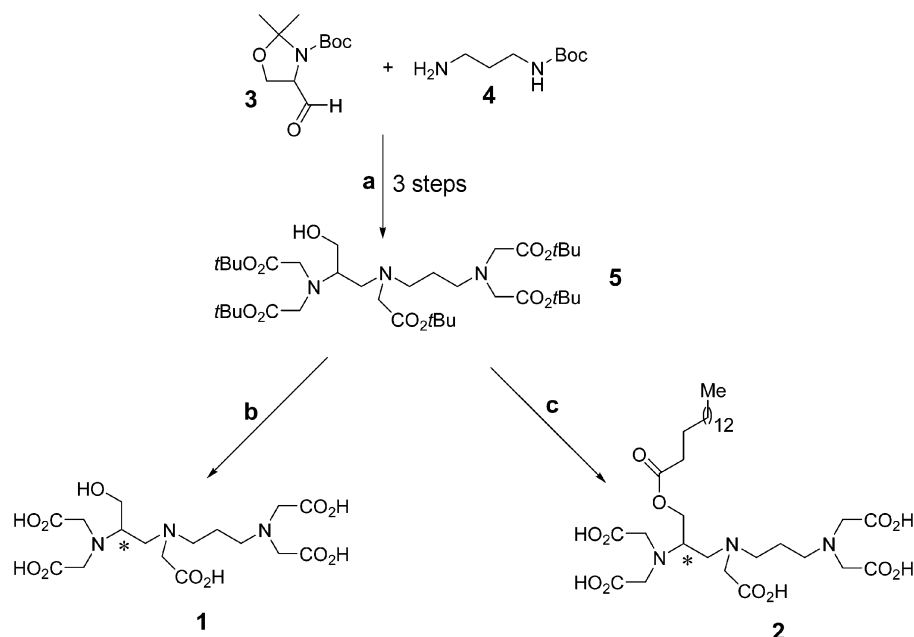
Scheme 1. (a) ref.[22] (b) 6M HCl/EtOH (1:1). (c) ref.[23]

tution of an ethylene by a propylene bridge on the DTPA skeleton is aimed at imposing steric compression around the water binding site, and therefore, to lead to Gd^{III} complexes with fast water-exchange rates. The hydroxymethyl "handle" is ideal for conjugation of the key protected intermediate **5** (Scheme 1) to organic moieties for targeting and/or τ_r optimization purposes. As *proof of concept* we have recently reported the synthesis and characterization the new micellar contrast agent [Gd(EPTPAC16)(H₂O)]^{2–}.[23]

Acidic deprotection of the fully protected intermediate **5** affords in quantitative yields the new chelator H₅EPTPA-CH₂OH (**1**) [Scheme 1]. The synthesis started with the unnatural *R* enantiomer of serine (D-Serine), and it is reasonable to assume that the synthetic route devised is not likely to have led to racemization or inversion of configuration on the stereogenic center. Ligand **1** displays a stereogenic center that is assumed to have an absolute *S* configuration. The apparent inversion of configuration $R \rightarrow S$ reflects only a change in the assignment of priority of one of the groups attached to the stereogenic center. The enantiomer excess could have been determined for the fully protected intermediate **5** through, for example, the MTPA ester method.[24] Although the enantiomeric excess was not measured, the obtained $[a]_D$ values of –31.9 (c = 1.0, H₂O, pH = 1.40) and –6.3 (c = 1.0, H₂O, pH = 9.8) confirm that the fully deprotected compound **1** is optically active. The dramatic difference in the measured $[a]_D$ values under acidic and basic conditions probably reflects the rigidity of the ligand in acidic media, which results from intramolecular hydrogen bonding.

Potentiometric Determination of Protonation and Stability Constants

The protonation constants of the ligands EPTPA-CH₂OH^{5–} and EPTPAC16^{5–} were determined by pH potentiometric titrations (Figure 2). The protonation constants of the two ligands, pK_i = log K_i^H, where K_i^H is defined as in Equation (1), are listed and compared to those of similar ligands and DTPA in Table 1 (standard deviations are shown in parenthesis).

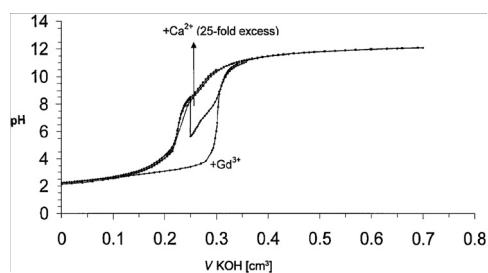$$K_i^H = [H_iL]/[H_{i-1}L][H^+]; \ i = 0,1,2,3,4,5 \tag{1}$$

Figure 2. Potentiometric pH titration curves for the ligand EPTPA-CH₂OH^{5–} in the absence and in the presence of Ca^{II} or Gd^{III} [c(EPTPACH₂OH) = 2.055 mM, c(KOH) = 0.2461 M, metal/ligand ratio = 1:1, I = 1.0 M KCl, T = 25 °C].

Both EPTPACH₂OH^{5–} and EPTPAC16^{5–} ligands display a slightly higher protonation constant for the first protonation step than that for the ligand DTPA^{5–[25]}, as observed previously for the unsubstituted ligand EPTPA^{5–[26]} and the backbone substituted EPTPA-bz-NO₂^{5–[20c]} (see Table 1). Such an increase in the protonation constants relative to those for DTPA^{5–} also occurs for the subsequent protonation steps for all the backbone substituted ligands, including the two studied in this work. This general increase in the protonation constants upon replacement of one ethylene group in the backbone of DTPA^{5–} by one trimethylene group results from reduced electrostatic repulsion between the protonated amino groups on lengthening of the chain between them.[26] The most pronounced increase is ob-

Table 1. Protonation constants for the ligands H_5EPTPACH$_2$OH (**1**) (25 °C, I = 1.0 M KCl) and H_5EPTPAC16 (**2**) (25 ± 0.2 °C, I = 0.1 M) and stability constants for the Gd^{III}–EPTPACH$_2$OH complex (25 °C, I = 1.0 M KCl). Data for other ligands are included for comparison.

	H_5DTPA[25]	H_5EPTPA-bz-NO$_2$[20c]	H_5EPTPA[26]	H_5EPTPACH$_2$OH[a]	H_5EPTPAC16[a]
pK_1	10.41	10.86(±0.01)	10.60	10.65(±0.08)	11.04(±0.01)
pK_2	8.37	8.91(±0.02)	8.92	8.39(±0.09)	8.91(±0.02)
pK_3	4.09	4.70(±0.02)	5.12	4.43(±0.09)	5.41(±0.03)
pK_4	2.51	3.25(±0.02)	2.80	2.78(±0.10)	5.02(±0.02)
pK_5	2.04	2.51(±0.03)	[c]	2.75(±0.08)	2.66(±0.08)
log K_{GdL}	22.50	19.20 (±0.02)	22.77[b]	16.7(±0.05)	[c]
log K_{GdHL}	1.80	3.40(±0.02)	[c]	3.64(±0.04)	[c]

[a] This work. [b] In ref.[20c] the corrected values for [Gd(EPTPA)(H$_2$O)]$^{2-}$ were found: log K_{GdL} = 18.75(±0.07) by direct titration and log K_{GdL} = 17.5 (±0.3) by competition with EDTA. [c] Not determined.

served for the third and fourth protonation steps for the ligand EPTPAC16^{5-}. This agrees with the fact that polyamines with increasing chain length usually display increasing protonation constants.[27]

The first protonation constant for the ligands EPTPA^{5-} and EPTPACH$_2$OH^{5-} is practically the same (within experimental error). The protonation constants for the other protonation steps are slightly lower for EPTPACH$_2$OH^{5-} than those observed for EPTPA^{5-}. The first four protonation constants of the ligand EPTPAC16^{5-} are higher than those of the nonconjugated ligand EPTPACH$_2$OH^{5-}. A rather pronounced effect is observed for the fourth protonation constant of EPTPAC16^{5-} – its value is two orders of magnitude higher than the corresponding value for EPTPA-CH$_2$OH^{5-}.

The stability and the protonation constants of the metal complexes are expressed in Equation (2) and Equation (3).

$$K_{ML} = [ML]/[M][L] \qquad (2)$$

$$K_{MH_iL} = [MH_iL]/[MH_{i-1}L][H^+]; \; i = 1,2 \qquad (3)$$

These thermodynamic stability constants, obtained by pH potentiometry for the Gd^{III}–EPTPACH$_2$OH system (Figure 2), are also listed in Table 1 and compared to those for the Gd complexes of similar ligands and DTPA. The species distribution diagram for the system Gd^{III}/EPTPA-CH$_2$OH/(H$^+$), represented in Figure 3, indicates that above pH 5, there is no free Gd^{III} in a solution containing a 1:1 molar ratio of Gd^{III} and ligand. The unprotonated complex [Gd(EPTPACH$_2$OH)(H$_2$O)]$^{2-}$ is the only species present at physiological pH 7.4. For the ligand EPTPAC16^{5-}, the observation of precipitation in the system for pH values below 4 precluded the determination of the stability constants of its Gd^{III} complex.

The value previously determined for the complex [Gd(EPTPA)(H$_2$O)]$^{2-}$ (log K_{GdL} = 22.77) from a competition study with EDTA^{4-}[26] is about the same as that measured for [Gd(DTPA)(H$_2$O)]$^{2-}$. This value did not seem reasonable because of the fact that EPTPA complexes form one six-membered chelates, which are less stable than the five-membered rings observed for the DTPA analogues. We therefore would have expected a lower stability for the EPTPA complexes. This was indeed demonstrated by Merbach et al.,[20c] who found, for [Gd(EPTPA)(H$_2$O)]$^{2-}$, a
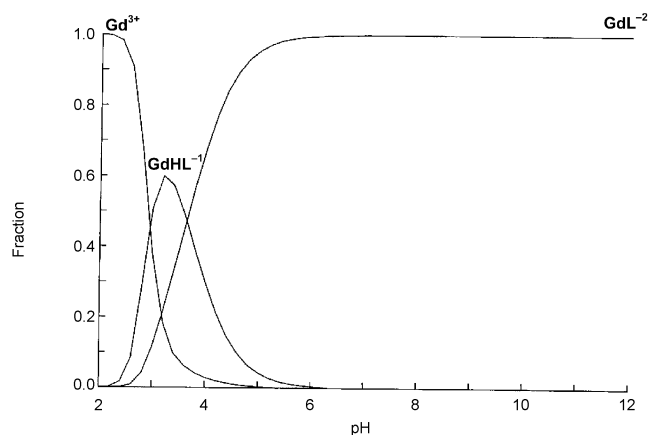

Figure 3. Species distribution curves for a 2 mM Gd^{III}/EPTPA-CH$_2$OH/(H$^+$) system containing a 1:1 molar ratio of Gd^{III} to ligand (I = 1.0 M KCl, T = 25 °C). Fraction is relative to 2 mM total Gd^{III} species.

value log K_{GdL} = 18.75(±0.07) by direct titration and log K_{GdL} = 17.5(±0.3) by competition with EDTA. The value log K_{GdL} = 16.7 ± 0.05 obtained in the present study for the thermodynamic stability constant of the complex [Gd(EPTPACH$_2$OH)(H$_2$O)]$^{2-}$ is two orders of magnitude lower than the corrected value for [Gd(EPTPA)(H$_2$O)]$^{2-}$ and even lower than the value for the complex [Gd(EPTPA-bz-NO$_2$)(H$_2$O)]$^{2-}$,[20c] which indicates the destabilizing effect of the CH$_2$OH substituent group at the EPTPA backbone. All these substitutions occur at the C4 position (position b, see Figure 1) of the EPTPA backbone, which might not be optimal for the stability of the complex; however, this depends on the type of substituent. It has been shown that substitution at the EPTPA backbone with a phenyl group has a stabilizing effect on the [Gd(EPTPA)(H$_2$O)]$^{2-}$ structure towards Zn^{2+} transmetallation; the effect is much higher when the substitution is at C9 than at C4 (positions b and f, respectively, see Figure 1), but substitution with a methyl group at C9 or C4 has no stabilizing effect on the parent compound.[28]

The present results, summarized in Table 1, show that the stability of the Ln^{III} complexes of the EPTPA derivatives decreases when the sum of the protonation constants of the free ligand increases, which is the opposite of the usual

trend found for many polyamino–polycarboxylic acids.[29] The trend can be explained by the presence of an extra CH$_2$ group in the ligand backbone, which increases the basicity of the adjacent nitrogen donor atoms, but reduces the stability of the six-membered chelate ring formed.

NMR pH Titrations

The macroscopic protonation constants obtained by potentiometry give no information on the microscopic sequence of protonation of the ligand sites. This protonation sequence can be obtained by ^{1}H NMR pH titration, where the chemical shifts of the ligand methylene protons are determined as a function of the pH, since the protonation of a basic site of a poly(aminocarboxylate) ligand results in a deshielding of the adjacent nonlabile methylene protons.[30] Changes in chemical shifts can quantitatively indicate the site of protonation.[30,31]

The ^{1}H NMR pH titration curves for some of the protons of the ligands H$_5$EPTPACH$_2$OH and H$_5$EPTPAC16 are shown in Figure 4. The corresponding resonances were assigned at different pH values on the basis of signal multiplicities, the signal crossovers, and COSY spectra in the whole pH range studied. These titration curves display sharp changes at different pH values, which relate to the protonation states of the ligand. Since there is fast exchange on the NMR time scale among the various protonated species (H$_n$L), the observed shift of a given proton is given by the average of the shifts of the various species (δ_{H_nL}) weighted by their molar fractions (x_n); $\delta_{obs} = \Sigma x_n \cdot \delta_{H_nL}$.[30] The procedure used to obtain the protonation fractions at each ligand site has been described in detail.[31] In summary, the shifts of the protonated species (δ_{H_nL}), obtained by fitting the experimental pH titration curves by using the potentiometric protonation constants, were used to calculate the protonation fractions (%) at the nitrogen [$f_N = f_{(1)}$, $f_{(2)}$, $f_{(3)}$] and oxygen [$f_O = f_{(4)}$, $f_{(5)}$, $f_{(6)}$] atoms (labelled in Figure 1) of each ligand protonation state H$_n$L (integer n = 1, 2, 3,... is the number of moles of acid added per mole of ligand). It was assumed that the protonation shifts at the various sites are additive, with a total shift ($\Delta\delta$) given by the expression $\Delta\delta = \Sigma C_N \cdot f_N + \Sigma C_{N'} \cdot f_N + \Sigma C_O \cdot f_O$, where C_N = 0.75 ppm, $C_{N'}$ = 0.35 ppm and C_O = 0.20 ppm are pH-independent shielding constants valid for linear poly(aminocarboxylate) ligands.[30]

The values of f_N [$f_{(1)}$, $f_{(2)}$, $f_{(3)}$] and f_O [$f_{(4)}$, $f_{(5)}$, $f_{(6)}$] were calculated for the H$_n$L species of the two ligands and compared with those reported for H$_5$EPTPA[26] (see Table S3 in the Supporting Information). The first two protonations occur in all cases exclusively at the backbone nitrogen atoms [$f_O = f_{(4)}$, $f_{(5)}$, $f_{(6)}$ = 0]. The f_i values for n = 1 show that the first protonation is very similar for the three ligands, where the more basic central nitrogen atom [N$_{(2)}$] is protonated preferentially to the terminal ones, as was also found for DTPA.[26,30,31] For n = 2, there is a preference for the protonation of the terminal nitrogen atoms over that of the central nitrogen atom in all ligands. However, the
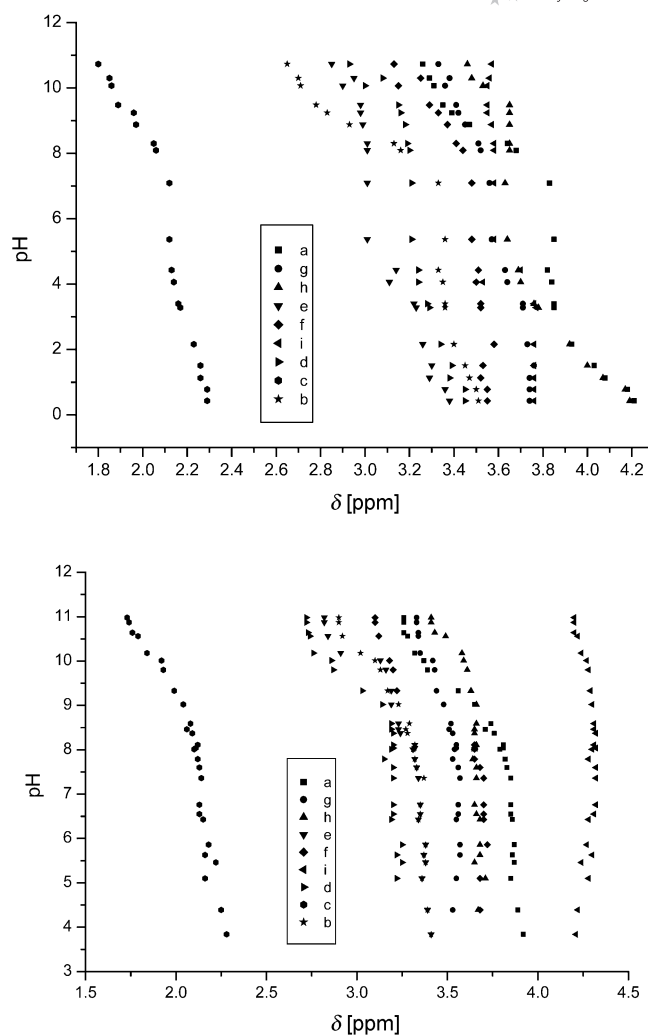

Figure 4. Variation of the ^{1}H NMR chemical shifts versus pH for the ligands H$_5$EPTPACH$_2$OH (top) and H$_5$EPTPAC16 (bottom) [see Figure 1 for the labelling of protons].

protonation of the two terminal nitrogen atoms is quite distinct in the three asymmetric ligands EPTPA and the two derivatives studied in this work. The protonation of the trimethylene nitrogen atom [N$_{(1)}$] is favored over that of the ethylene nitrogen atom [N$_{(3)}$] for n = 1–3, because of the increased separation in the positive charges in N$_{(1)}$–N$_{(2)}$ relative to N$_{(2)}$–N$_{(3)}$ and possibly also because of the stabilization of a six-membered ring by hydrogen bonding between N$_{(1)}$ and N$_{(2)}$. The protonation of N$_{(3)}$ is less favored in the two EPTPA derivatives than in EPTPA because of the steric effect of the C4-substituents in the ethylenediamine moiety. The forms with the protonated terminal nitrogen atoms are stabilized by internal hydrogen bonding with the corresponding carboxylate groups, which leads to increased values for the second and third protonation constants relative to those for DTPA.[26,30,31] These internal hydrogen bonds also lead to preferential protonation of the carboxylate groups bound to the less protonated nitrogen atoms, as shown by the f_i values, which could be obtained for n > 2.

^{1}H NMR Study of [Ln(EPTPACH$_2$OH)]$^{2-}$ Complexes

The ^{1}H NMR spectra of the [Ln(EPTPACH$_2$OH)]$^{2-}$ complexes, both diamagnetic (Ln = La, Lu, Y) and paramagnetic (Ln = Pr, Nd, Sm, Eu, Tb, Dy, Yb), were obtained in D$_2$O at pH 7.0 as a function of temperature (7, 25, 60 and 80 °C; see Figure S1 in the Supporting Information for some typical spectra). The diamagnetic spectra (illustrated in Figure S1a by the Y^{III} complex) are quite crowded and were not fully assigned. The presence of high and low intensity resonances could be seen throughout the whole spectrum for all the diamagnetic complexes. The COSY spectrum of [Y(EPTPACH$_2$OH)]$^{2-}$ (Figure S2a, Supporting Information) contains two sets of five cross peaks of high and low intensity, which correspond to the five AB quartets characteristic of the methylene protons of the five bound acetate groups of EPTPA in two isomeric complexes of high and low populations. The signals for the Lu^{III} and Y^{III} complexes did not broaden significantly at high temperatures. This is not the case for the La^{III} complex, whose signals becomes very broad at high temperature, as found for the La^{III}- and Lu^{III}–DTPA complexes, in which the central nitrogen racemization process is quite effective, and therefore, the spectra of the two asymmetric conformers present is effectively averaged.[32,33]

All the ^{1}H NMR spectra of the paramagnetic complexes studied also show high and low intensity resonances. This is best seen in the sharper spectra of the early-Ln^{III} series (see Figure S1b,c,d), which confirms the presence of two isomeric complexes, one of much higher population than the other. The major complex, whose spectrum exhibits 21 resonances of high intensity, has a smaller spread of proton paramagnetic shifts than that of the low intensity resonances of the minor complex. The presence of one resonance per nonexchangeable ligand proton shows that racemization of the central nitrogen through the wagging of the attached acetate group does not occur. Again, a different result is observed for the spectra of the paramagnetic Ln^{III}–DTPA complexes, where racemization of the central nitrogen through a wagging motion of its bound acetate group averages the spectra of the two asymmetric conformers present in solution.[34,35]

All the paramagnetic spectra were too complex to be assigned, even with the help of observable COSY cross peaks (Figure S2b,c). The signals from the major isomer were not significantly broadened at high temperatures, in contrast to those from the minor isomer. This is most clearly observed for the spectrum of the Sm^{III} complex (Figure S1c), with a major/minor ratio of 25:4, in which the broadening of the three high-frequency doublets (7.66, 7.27, and 6.85 ppm) at 40 °C makes the couplings unobservable. Further, of the three low-frequency multiplets, the one at –2.02 ppm is selectively broadened at 40 °C. The major and minor isomers observed in the [Ln(EPTPACH$_2$OH)]$^{2-}$ complexes result from the conformational properties of the ligand backbone. While the six-membered ring formed by the Ln^{III}–propylenediamine chelate is locked in a chair conformation,[36] the ethylenediamine moiety can adopt a δ or λ conformation in its five-membered ring chelate. One of these conformations places the CH$_2$OH substituent in a more stable, less-crowded position than that in the other conformation. The CH$_2$OH substituent prevents the central acetate wagging motion and also slows down the δ/λ backbone interconversion process that averages the spectra of the major (M) and minor (m) complexes. The selective broadening of the signals of minor complex that results from this dynamic process is a consequence of the equilibrium constant K_{eq} = [m]/[M] $\ll$ 1 being unfavorable to the m species, which leads to relative kinetic constants k(m→M) $\gg$ k(M→m).

^{17}O NMR, ^{1}H NMRD and EPR Measurements

The water-exchange rate was determined for the Gd^{III}–EPTPACH$_2$OH^{5-} complex from a variable-temperature ^{17}O NMR spectroscopic study. Additionally, the magnetic field dependence of the longitudinal water proton relaxivities (r_1) [nuclear magnetic relaxation dispersion − NMRD − curves] at different temperatures and EPR spectra were measured on the same complex with the objective of determining the parameters that describe water exchange, rotation, electronic relaxation, and proton relaxivity.

The obtained experimental NMRD data (Figure 5) and the ^{17}O NMR chemical shifts ($\Delta\omega_r$), longitudinal ($1/T_{1r}$) and transverse ($1/T_{2r}$) relaxation rates (Figure 6) were analyzed simultaneously by using the Solomon–Bloembergen–Morgan (SBM) theory (for the equations used in the data analysis, see the Supporting Information). It was assumed that [Gd(EPTPACH$_2$OH)(H$_2$O)]$^{2-}$ had one inner-sphere water molecule (q = 1), as in the [Gd(EPTPA)(H$_2$O)]$^{2-}$ and [Gd(EPTPA-bz-NO$_2$)(H$_2$O)]$^{2-}$ complexes.[20c] The parameters obtained in the fit are shown in Table 2, and Figures 5 and 6 show the corresponding fitted curves obtained for the NMRD and ^{17}O NMR spectroscopic data. The ratio of the rotational correlation times of the Gd–O and Gd–H vectors, τ_{rO} and τ_{rH}, respectively, fluctuated during the fits around its theoretical lower limit of 0.65 (based on geometrical considerations) and has been fixed to that value.[37] Some parameters given in Table 2 have been adjusted in preliminary fits and fixed in the final fitting procedure. Other parameters were fixed in the fit to typical values from the literature:[4,5] the ^{17}O scalar coupling constant $A/\hbar$ = –3.2 × 10^6 rad s^{-1}, the relative diffusion coefficient between the complex and water molecules D_{GdH}^{298} = 25 × 10^{10} m^2 s^{-1} and the corresponding activation energy E_{DGdH} = 25 kJ mol^{-1}, the distance of closest approach between the Gd^{III} ion and the outer-sphere water molecules a_{GdH} = 3.6 Å, the distances between Gd^{III} and the coordinated water oxygen atom r_{GdO} = 2.50 Å and protons r_{GdH} = 3.10 Å, the quadrupolar coupling constant for the bound water ^{17}O $\chi(1+\eta^2/3)^{1/2}$ = 7.68 MHz,[38] and the empirical constant for the outer-sphere contribution to the ^{17}O chemical shift C_{os} = 0.1.[20c] The values obtained for the activation parameters for water exchange, $\Delta H^{\ddagger}$ and $\Delta S^{\ddagger}$, and for the activation energies, E_v and E_R, are very close to those obtained for the [Gd(EPTPA)(H$_2$O)]$^{2-}$ and [Gd(EPTPA-bz-NO$_2$)(H$_2$O)]$^{2-}$ complexes (Table 2).[20c]
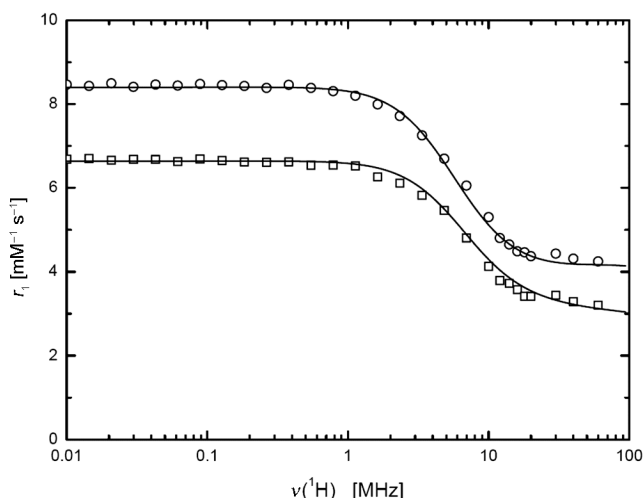
Figure 5. ^1H NMRD profiles at 25 °C (circles) and 37 °C (squares) for $[Gd(EPTPACH_2OH)(H_2O)]^{2-}$. The lines represent curves from results of a simultaneous fit of NMRD and ^{17}O NMR spectroscopic data.

Table 3 compares the values for the parameters that determine relaxivity – the water-exchange rate (k_{ex}^{298}), the rotational correlation time of the complex (τ_{rO}^{298}) and the electron spin relaxation parameters (Δ^2 and τ_V^{298}) – obtained for $[Gd(EPTPACH_2OH)(H_2O)]^{2-}$ with the corresponding values for Gd^III complexes with other ligands containing the EPTPA structure and with DTPA.[20c,23,39] The 20 MHz proton relaxivities obtained for those systems are also compared.[26] The water-exchange rate of $[Gd(EPTPA-CH_2OH)(H_2O)]^{2-}$, $k_{ex}^{298} = 87.6 \times 10^6$ s^{-1}, is consistent with values obtained for analogous chelates that form between Gd^III and EPTPA-based ligands and is close to the theoretically derived optimal value ($k_{ex}^{298} \approx 10^8$ s$^{-1[20c]}$). In all these compounds, steric compression around the water binding site leads to accelerated water exchange relative to DTPA-based Gd^III complexes.[20c,23] However, it is interesting to observe that, while the inclusion of substituents on the C4 carbon atom of the ethylene bridge of a series of Gd^III–DTPA complexes leads to a 3–5 fold increase in k_{ex}^{298} relative to that of the parent complex $[Gd(DTPA)(H_2O)]^{2-}$,[15–18] similar substitution on the C4 carbon atom of the ethylene bridge of a series of Gd^III–EPTPA complexes leads to a 2–4 fold decrease in k_{ex}^{298} relative to that of the parent complex $[Gd(EPTPA)(H_2O)]^{2-}$;[20c,23] $[Gd(EPTPA)(H_2O)]^{2-}$ has a k_{ex}^{298} value that is 100 times larger than that of $[Gd(DTPA)(H_2O)]^{2-}$. Another study has also shown that substitution by a methyl group at C4, and specially at C9 (propylene bridge), in the parent complex gives the highest k_{ex} values, but substitution by a bulkier phenyl group at both positions decreases the water-exchange rates to values only 3 times larger than that for Gd^III–DTPA.[28]

With regard to rotational dynamics, the rotational correlation time obtained for $[Gd(EPTPACH_2OH)(H_2O)]^{2-}$ is comparable to the values for other small Gd^III complexes, where the relative values increase, as expected, with their molecular weights. Therefore, the 20 MHz proton relaxivity
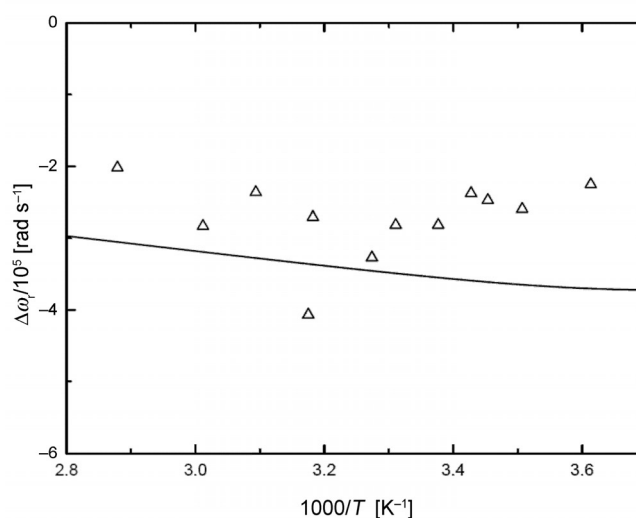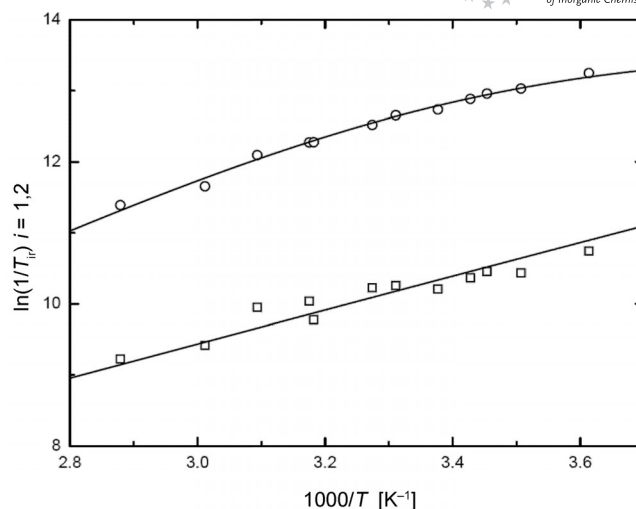

Figure 6. Temperature dependence of transverse and longitudinal ^{17}O relaxation rates (top) and ^{17}O chemical shifts (bottom) for $[Gd(EPTPACH_2OH)(H_2O)]^{2-}$ at $B = 4.7$ T. The lines represent curves from results of a simultaneous fit of NMRD and ^{17}O NMR spectroscopic data.

Table 2. Parameters obtained for the $[Gd(EPTPACH_2OH)(H_2O)]^{2-}$ chelate from the analysis of ^{17}O NMR and NMRD data (parameters in italics have been fixed in the final fit).

Parameter	
k_{ex}^{298} [10^6 s^{-1}]	87.6 ± 16.3
$\Delta H^{\ddagger}$ [kJ mol^{-1}]	30.5 ± 4.1
$\Delta S^{\ddagger}$ [J mol^{-1} K^{-1}]	$+9.4 \pm 10$
$A/\hbar$ [10^6 rad s^{-1}]	*–3.2*
τ_{rO}^{298} [ps]	116.2
E_R [kJ mol^{-1}]	19.8 ± 1.3
τ_V^{298} [ps]	8.8 ± 0.7
E_v [kJ mol^{-1}]	*1.0*
Δ^2 [10^{20} s^{-2}]	0.89 ± 0.10
D_{GdH}^{298} [10^{-10} m^2 s^{-1}]	*25*
E_{DGdH} [kJ mol^{-1}]	*25*
$\tau_{rH}^{298}/\tau_{rO}^{298}$	*0.65*

r_1 of the EPTPA-based Gd^III complexes, shown in Table 3, is determined by the (relatively fast) rotational correlation time, as is usual for all small complexes.

Table 3. Relaxivity (at 20 MHz and 25 °C) and parameters determining relaxivity for selected Gd[III] complexes.

Complex	k_{ex}^{298} [10^6 s^{-1}]	τ_{rO}^{298} [ps]	Δ^2 [10^{20} s^{-2}]	τ_V^{298} [ps]	r_1 [mM^{-1} s^{-1}]
[Gd(DTPA)(H$_2$O)]$^{2-}$[39]	3.3	58	0.46	25	3.89[26][c]
[Gd(EPTPA)(H$_2$O)]$^{2-}$[20c]	330	75	0.76	22.4	3.85[26][d]
[Gd(EPTPACH$_2$OH)(H$_2$O)]$^{2-}$[a]	87.6	116.2	0.4	22	4.37
[Gd(EPTPA-bz-NO$_2$)(H$_2$O)]$^{2-}$[20c]	150	122	0.89	8.8	4.73
[Gd(EPTPAC16)(H$_2$O)]$^{2-}$[23][b]	170	τ_{rH} = 200	0.08	44	9.11

[a] This work. [b] Monomer form. [c] At 37.0 ± 0.1 °C and pH = 7.6 ± 0.1. [d] At 37.0 ± 0.1 °C and pH = 7.5 ± 0.1.

In our combined analysis of the ^{17}O NMR and NMRD data, we used the simple Solomon–Bloembergen–Morgan (SBM) theory, which is known to give only a rough approximation for electron spin relaxation rates $1/T_{1e}$ and $1/T_{2e}$.[40–42] We will therefore not discuss the parameters linked to it (τ_v, Δ^2). X-band EPR spectra of the [Gd(EPTPACH$_2$OH)(H$_2$O)]$^{2-}$ complex in aqueous solution at 298 K gave an approximately Lorentzian line centered at a magnetic field corresponding to $g_L \approx 2.0$, with an experimental peak-to-peak linewidth ΔH_{pp} = 23.64 ± 0.05 mT. The value for the linewidth was independent of the concentration of the complex in the range studied. The corresponding transverse electronic relaxation rate ($1/T_{2e}$) was calculated using Equation (4), in which the symbols have their usual meaning.[43]

$$\frac{1}{T_{2e}} = \frac{g_L \mu_B \pi \sqrt{3}}{h} \Delta H_{pp} \qquad (4)$$

The calculated transverse electron spin relaxation rate of $(1/T_{2e})_{exp} = 2.265 \times 10^{10}$ s^{-1} (at B = 0.34 T) is about three times larger than $(1/T_{2e})_{calc} = 7.14 \times 10^9$ s^{-1}, the value calculated by using Morgan's equation (A20, Supporting Information) with Δ^2 and τ_V^{298} obtained from the simultaneous fitting of the ^{17}O NMR and ^{1}H NMRD data (Table 3). X-band experimental EPR values of $1/T_{2e}$ have been systematically found to be larger than those calculated for many Gd[III] complexes, which confirms the deficiencies of SBM theory.[31,43,44,45] The use of a more recent description of electron spin relaxation needs, however, EPR measurements to be made over a wide temperature range and with different frequencies.[46]

Transmetallation Kinetics

The kinetic stability of [Gd(EPTPACH$_2$OH)(H$_2$O)]$^{2-}$ in solution towards transmetallation with Zn^{2+} was evaluated by the time dependence of the decrease in the water proton longitudinal relaxation rate (R_1^p) of phosphate-buffered solutions containing Zn^{2+}.[47] Precipitation as phosphates of the Gd^{3+} ions released as a result of substitution by Zn^{2+} leads to a decrease in R_1^p that is proportional to the amount of released Gd^{3+} ions. In the absence of Zn^{2+}, the stability of the Gd^{3+} complex in the phosphate buffer depends on the buffer concentration, and is much higher at 10 mM than at 67 mM (Figure 7). The kinetic stability in the

concentrated buffer is similar to the behavior observed for [Gd(4-Me-EPTPA) (H$_2$O)]$^{2-}$.[28] In the presence of Zn^{2+}, the decrease in R_1^p is much faster, which indicates a fast and extensive transmetallation process (Figure 7). The rate and extent of this process increases with buffer concentration. However, at higher buffer concentrations, the kinetic stability of [Gd(EPTPACH$_2$OH)(H$_2$O)]$^{2-}$ towards Zn^{2+} transmetallation is higher than that of [Gd(4-Me-EPTPA) (H$_2$O)]$^{2-}$, but is still much lower than that of C9- and C4 phenyl-substituted [Gd(EPTPA)(H$_2$O)]$^{2-}$ derivatives.[28]
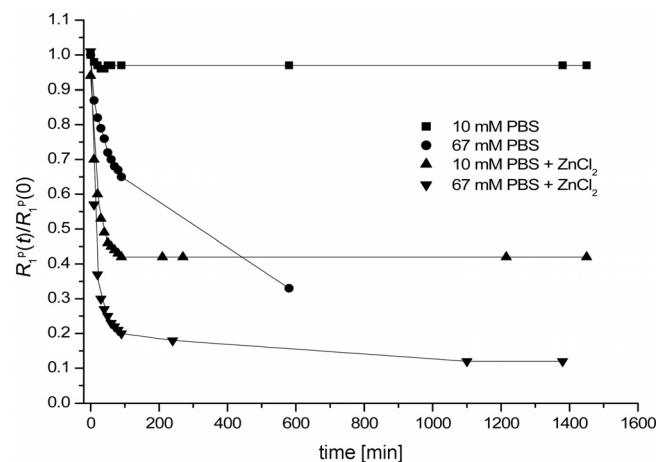

Figure 7. Time evolution of the proton relaxation rate of 2.5 mM [Gd(EPTPACH$_2$OH)(H$_2$O)]$^{2-}$ (20 MHz, 310 K, pH 7.1) in (■) 10 mM PBS, (●) 67 mM PBS, (▲) 10 mM PBS and 2.5 mM of ZnCl$_2$, and (▼) 67 mM PBS and 2.5 mM of ZnCl$_2$.

Conclusions

We have devised a new synthetic route to the ligand 4-(S)-hydroxymethyl-3,6,10-tri(carboxymethyl)-3,6,10-triaza-dodecanoic acid, H$_5$EPTPACH$_2$OH. The fully protected precursor compound **5** is a versatile block for conjugation to biological moieties for targeting purposes and/or optimization of τ_r, as demonstrated before.[23] The hydroxymethyl group allows the construction of potentially responsive contrast agents through enzymatic activation of cleavable bonds such as ester, phosphodiester, and glycosidic bonds. Moreover, although we have not attempted to functionalize the complex of the deprotected ligand **1**, we envisage that this could be an interesting approach to the (enzymatic) synthesis of conjugates that cannot resist the usual harsh deprotection conditions.

Potentiometry studies reveal that the ligand displays slightly higher protonation constants relative to those for the ligand DTPA$^{5–}$, which is consistent with the fact that polyamines with increasing chain length usually display increasing protonation constants. NMR pH titrations give some insight into the ligand microscopic protonation scheme. The first protonation occurs at the more basic central nitrogen atom preferentially over the terminal ones, as was also found for DTPA$^{5–}$. In the second protonation step, there is a preference for the terminal trimethylene and ethylene nitrogen atoms over the central nitrogen atom. Moreover, protonation at the ethylene nitrogen atoms is less favored because of the steric effect of the C4 substituents.

The stability constant (log K_{GdL} = 16.7) for the [Gd(EPTPACH$_2$OH)(H$_2$O)]$^{2–}$ complex is two orders of magnitude lower than that for the [Gd(EPTPA)(H$_2$O)]$^{2–}$ complex, which indicates the destabilizing effect of the CH$_2$OH group on the EPTPA backbone.

^{1}H NMR studies of the Ln^{III} chelates of these ligands in aqueous solution unambiguously show two sets of high and low intensity resonances, despite being too complex to be assigned, which confirms the presence of two isomeric complexes, one of much higher population than the other.

The water-exchange rate obtained for [Gd(EPTPA-CH$_2$OH)(H$_2$O)]$^{2–}$ is close to the theoretically derived optimal value that gives the highest proton relaxivities of Gd^{III}-based contrast agents. Despite the optimization of the water-exchange rate, the corresponding proton relaxivities are limited by a far from optimal rotational correlation time.

This ligand offers the possibility for conjugation of slowly rotating moieties through the hydroxymethyl handle, therefore this allows the design of Gd^{III}-based contrast agents with simultaneous optimization of the water-exchange rate and rotational correlation time. This approach has been previously applied to the synthesis of the [Gd(EPTPAC16)(H$_2$O)]$^{2–}$ complex.[23]

The kinetic stability of [Gd(EPTPACH$_2$OH)(H$_2$O)]$^{2–}$ in phosphate-buffered solutions towards Zn^{2+} transmetallation is quite low, but higher than that of [Gd(4-Me-EPTPA)(H$_2$O)]$^{2–}$.[28]

Experimental Section

Materials and Equipment: Chemicals of the highest analytical grade were purchased from Sigma–Aldrich and were used without further purification. Solvents used were of reagent grade and purified by the usual methods. Reactions were monitored by TLC on Kieselgel 60 F$_{254}$ (Merck) and products were detected by examination under UV light (254 nm) and by adsorption of iodine vapor. ^{1}H and ^{13}C NMR spectra (assigned by 2D DQF-COSY and HMQC techniques) were recorded with a Varian Unity Plus 300 NMR spectrometer operating at 299.938 MHz and 75.428 MHz for ^{1}H and ^{13}C, respectively. For ^{1}H and ^{13}C NMR spectra recorded in D$_2$O, chemical shifts (δ) are given in ppm relative to sodium 3-(trimethylsilyl)propanesulfonate (TSP) as internal reference (^{1}H, δ = 0.0 ppm) and *tert*-butanol as external reference (^{13}C, CH$_3$ δ = 30.29 ppm). ^{13}C NMR spectra were proton broad-band decoupled by using a GARP-1 modulated decoupling scheme. Mass spectrometry mea-

surements were performed with an APEX III FT-ICR MS (Bruker Daltonics, Billerica, MA), equipped with a 7-T actively shielded magnet. Ions were generated by using an Apollo API electrospray ionization (ESI) source (Bruker Daltonics, Billerica, MA). Samples were prepared by applying a spray solution of 50:49.5:0.5 (v/v/v) water/methanol/formic acid at a v/v ratio of 1 to 5%. Data acquisition and data processing were performed with the XMASS software, version 6.1.2 (Bruker Daltonics).

Synthesis and Characterization

Compounds 2, 3, 4 and 5: The synthesis of compounds **2**, **3**, **4**, and **5** was described previously by us.[23]

Compound 1: Purified compound **5** (2.32 g, 5.98 mmol) was stirred overnight at room temperature with 6 M HCl/EtOH (1:1, 40 cm^3) to afford the title compound in a quantitative yield. As the precursor, fully protected compound **5** was of analytical purity, as demonstrated before,[23] no further purification of the deprotected final compound **1** was judged necessary. ^{1}H NMR (300 MHz, H$_2$O, pH = 5.26): δ = 2.14 (m, 2 H, NCH$_2$C*H*$_2$CH$_2$), 2.99–3.72 [m br., 9 H, overlapping signals from NC*H*$_2$CH$_2$C*H*$_2$; OHC*H*$_2$NC*H*C*H*$_2$N], 3.60 (s, 4 H, terminal acetate protons linked to the ethylene bridge), 3.65 (s, 2 H, central acetate protons), 3.87 (s, 4 H, terminal acetate protons linked to the propylene bridge) ppm. ^{13}C (5.6 MHz, D$_2$O): δ = 23.12 (NCH$_2$C*H*$_2$CH$_2$N), 54.11, 55.86, 56.30 and 57.78 (signals from NC*H*$_2$CH$_2$C*H*$_2$N and from HOC*H*$_2$CH*C*H$_2$), 56.70 [N(C*H*$_2$CO$_2$H)$_2$], 60.07 [N(C*H*$_2$CO$_2$H)$_2$], 61.73 (NC*H*$_2$CO$_2$H, central acetate), 63.68 (NC*H*CH$_2$N), 173.32, 175.92 and 180.22 (*C*O$_2$H) ppm. HRMS (ESI$^+$): calcd. for C$_{16}$H$_{28}$N$_3$O$_{11}$ [M + H]$^+$ 438.1725680; found 438.1718352.

Protonation and Stability Constants Determined by Potentiometry

Ligand protonation constants were determined at constant ionic strengths [1.0 M KCl for H$_5$EPTPACH$_2$OH and 0.1 M (CH$_3$)$_4$NCl for H$_5$EPTPAC16]. The ligand solutions (5 cm^3 H$_5$EPTPACH$_2$OH and 3 cm^3 H$_5$EPTPAC16), stirred continuously, were titrated in a thermostatted cell (25 ± 0.2 °C) under a constant stream of N$_2$ by using 0.25 M (H$_5$EPTPACH$_2$OH) and 0.05 M (H$_5$EPTPAC16) standardized solutions of KOH as the titrants in a Metrohm Dosimat 776 and 665 automatic burette. Combined glass electrodes (Metrohm 6.0234.100 and C14/02-Sc, Ag/AgC1 reference electrode in 3 M KCl; Moeller Scientific Glass Instruments, Switzerland) connected to a Radiometer pHM93 reference pH meter and Metrohm 692 pH/ion meter were used to measure the pH. Protonation constants were determined at 0.002 M and 0.003 M ligand concentrations from two-two parallel titrations. The exact concentration of the H$_5$EPTPACH$_2$OH stock solution was also determined potentiometrically. During the ligand titration, after the observation of the first equivalent point, a 25-fold excess of Ca^{II} ions were injected into the sample. The large excess of Ca^{II} liberated the protons that remained on the ligand, and a second equivalent point was observable. The two ligand equivalent protons between the two equivalent points can be determined (see Figure 2). For determination of the stability constants of the [Gd(EPTPACH2OH)-(H$_2$O)]$^{2–}$ complex, solutions containing the ligand and Gd^{III} in equimolar concentrations were titrated directly with KOH. The hydrogen ion concentration was calculated from the measured pH values by using the correction method suggested by Irving et al.[48] Data treatment and processing was done with the program PSEQUAD.[49]

NMR pH Titrations

Solutions of the ligands (11.8 mM) for NMR pH titrations were made in D$_2$O (99.8%), and the pD was adjusted with DCl or CO$_2$-free NaOD. The final pD values were measured on a HANNA

8417 pH meter with a HI1310 combined electrode (HANNA instruments, Italy) and converted to pH values by using the isotopic correction pH = pD – 0.4.[50] ^{1}H NMR (1D and 2D COSY) spectra for the pH titrations were carried out with a Varian Unity Plus 300 NMR spectrometer operating at 299.938 MHz at a probe temperature of 25 ± 0.5 °C. Chemical shifts (δ) are given in ppm relative to TSP as internal reference.

^{1}H NMR of [Ln(EPTPACH$_2$OH)]$^{2-}$: To an aqueous solution of the ligand (pH = 5.0) was added dropwise an aqueous solution of the corresponding LnCl$_3$ in a 1:1 mol ratio. The pH was kept at about 5.0 by the addition of aqueous KOH, and the solution was stirred at room temperature for 1 h. The pH was then adjusted to 7.0 by the addition of KOH (aqueous solution). The solution was concentrated under reduced pressure. The solutions for NMR measurements were obtained by dissolution of the solid complexes obtained previously in D$_2$O ($V = 1$ cm^3) to obtain 30 mM concentrations. Proton 1D and 2D COSY spectra of the solutions of the diamagnetic (La^{III}, Lu^{III}, and Y^{III}) and paramagnetic (Pr^{III}, Nd^{III}, Sm^{III}, Eu^{III}, Tb^{III}, Dy^{III}, and Yb^{III}) complexes were obtained at 7, 25, 60, and 80 °C with Varian Unity Plus 300 (299.938 MHz) and Varian Unity 500 (499.826 MHz) NMR spectrometers.

^{17}O NMR, NMRD and EPR Experiments

Sample Preparation: The Gd^{III} chelate of EPTPACH$_2$OH (for ^{17}O NMR and NMRD) was prepared by mixing equimolar amounts of GdCl$_3$ and the ligand. A slight excess (5%) of ligand was used, and the pH of the stock solution was adjusted by adding aqueous NaOH (0.1 mM). The solution was allowed to react for 1 h at room temperature. The absence of free metal was checked in each sample by testing with xylenol orange.[51] ^{17}O-enriched water (^{17}O: 11.4%) was added to the solutions for the ^{17}O measurements to improve the sensitivity. The final solution concentration was 25.39 mmol kg^{-1} at pH 6.89. For the NMRD experiments, 6.99 mM solutions at pH 6.18 were used.

^{17}O NMR Experiments: Variable-temperature ^{17}O NMR measurements were performed with a Bruker Avance-200 (4.7 T, 27.1 MHz) spectrometer, and a BVT-3000 temperature-control unit was used to stabilize the temperature that was measured by a substitution technique. The samples were sealed in glass spheres that fitted into 10-mm o.d. NMR tubes to eliminate susceptibility corrections to the chemical shifts.[52,53] Longitudinal relaxation rates $1/T_1$ were obtained by the inversion recovery method, and transverse relaxation rates $1/T_2$ by the Carr–Purcell–Meiboom–Gill spin-echo technique. As an external reference, acidified water of pH 3.4 was used.

NMRD Measurements: The measurements were performed by using a Stelar Spinmaster FFC NMR relaxometer (0.01–20 MHz) equipped with a VTC90 temperature control unit. At higher fields, the ^{1}H relaxivity measurements were performed with Bruker Minispecs mq30 (30 MHz), mq40 (40 MHz), and mq60 (60 MHz) instruments. In each case, the temperature was measured by a substitution technique. Variable-temperature measurements were performed at 25 and 37 °C.

EPR Spectroscopy: The X-band (0.34 T, 9.4 GHz) EPR spectra were recorded with a Bruker ESP 300E spectrometer. The spectra were recorded at 25 °C on a quartz flat cell at four different concentrations (23 mM, 10 mM, 5 mM, 1 mM) of aqueous [Gd(EPTPA-CH2OH)(H$_2$O)]$^{2-}$, pH 6.8 The frequency was calibrated with diphenyl picrylhydrazyl (dpph), and the magnetic field with Mn^{II} in MgO. The transverse electronic relaxation rates, $1/T_{2e}$, were calculated from the EPR linewidths according to Reuben.[54]

Transmetallation: Transmetallation by Zn^{2+} ions was evaluated by the decrease in the water proton longitudinal relaxation rate, at 310 K and 20 MHz (Bruker Minispec mq20), of phosphate-buffered solutions (PBS, pH 7.1, 10 mM or 67 mM) containing 2.5 mM of [Gd(EPTPACH$_2$OH)(H$_2$O)]$^{2-}$ and 2.5 mM of ZnCl$_2$.[47] The water longitudinal relaxation rate was also measured on PBS-buffered solutions (pH 7.1, 10 mM and 67 mM) containing 2.5 mM of [Gd(EPTPACH$_2$OH)(H$_2$O)]$^{2-}$.[28]

Data Analysis: The simultaneous least-squares fittings of the ^{17}O NMR and NMRD relaxation data were performed with the Visualiseur/Optimiseur programs on a Matlab platform version 6.5.[55]

Supporting Information (see footnote on the first page of this article): Equations used for the determination of the relaxivity parameters from the analysis of NMRD and ^{17}O NMR spectroscopic data; Tables used for the determination of the microscopic protonation scheme of the ligands, which contain the pH dependence of the proton chemical shifts for H$_5$EPTPACH$_2$OH (Table S1) and H$_5$EPTPAC16 (Table S2), Table detailing the calculated percent protonation fractions of the different basic sites of H$_5$EPTPA-CH$_2$OH and H$_5$EPTPAC16 for different values of n (for identification of f_n sites see Figure 1) and listing the reported values for H$_5$EPTPA (Table S3), Tables containing the frequency dependence of the water proton relaxivities of [Gd^{III}(EPTPACH$_2$OH)(H$_2$O)]$^{2-}$ at two temperatures (Table S4), and the variable temperature reduced transverse and longitudinal ^{17}O relaxation rates and chemical shifts of [Gd(EPTPACH$_2$OH)(H$_2$O)]$^{2-}$ solution at 4.7 T (Table S5); 300 MHz ^{1}H NMR spectra of [Ln(EPTPACH$_2$OH)]$^{2-}$ complexes in D$_2$O (30 mM, pH 7.0, $T = 25$ °C): a) Nd^{III} complex, b) Eu^{III} complex, c) Sm^{III} complex, d) Y^{III} complex (Figure S1) and 500 MHz ^{1}H COSY spectra of [Ln(EPTPACH$_2$OH)]$^{2-}$ complexes in D$_2$O (30 mM, pH 7.0, $T = 25$ °C), from top to bottom: Y^{III} complex, Nd^{III} complex, Sm^{III} complex (Figure S2).

Acknowledgments

[1] R. B. Lauffer, *Chem. Rev.* **1987**, *87*, 901–927.

[2] S. Aime, M. Botta, M. Fasano, E. Terreno, *Chem. Soc. Rev.* **1998**, *27*, 19–29.

[3] P. Caravan, J. J. Ellison, T. J. McMurry, R. B. Lauffer, *Chem. Rev.* **1999**, *99*, 2293–2352.

[4] É. Tóth, L. Helm, A. E. Merbach, *Top. Curr. Chem.* **2002**, *221*, 61–101.

[5] *The Chemistry of Contrast Agents in Medical Magnetic Resonance Imaging* (Eds.: É. Tóth, A. E. Merbach), Wiley, Chichester, **2001**.

[6] a) É. Tóth, L. Helm, K. E. Kellar, A. E. Merbach, *Chem. Eur. J.* **1999**, *5*, 1202–1211; b) F. A. Dunand, É. Tóth, R. Hollister, A. E. Merbach, *J. Biol. Inorg. Chem.* **2001**, *6*, 247–255; c) M. G. Duarte, M. H. Gil, J. A. Peters, J. M. Colet, L. Vander Elst, R. N. Muller, C. F. G. C. Geraldes, *Bioconjugate Chem.* **2001**, *12*, 170–177.

[7] a) D. M. Corsi, L. V. Elst, N. Muller, H. van Bekkum, J. A. Peters, *Chem. Eur. J.* **2001**, *7*, 64–71; b) J. P. André, C. F. G. C. Geraldes, J. A. Martins, A. E. Merbach, M. I. M. Prata, A. C. Santos, J. J. P. de Lima, É. Tóth, *Chem. Eur. J.* **2004**, *10*, 5804–5816; c) P. Baía, J. P. André, C. F. G. C. Geraldes, J. A. Martins, A. E. Merbach, É. Tóth, *Eur. J. Inorg. Chem.* **2005**, 2110–2119.

[8] a) S. Aime, M. Fasano, E. Terreno, M. Botta in *The Chemistry of Contrast Agents in Medical Magnetic Resonance Imaging* (Eds.: É. Tóth, A. E. Merbach), Wiley, Chichester, **2001**, p. 193; b) S. Aime, M. Botta, S. G. Crich, G. Giovenzana, G. Palmisano, M. Sisti, *Bioconjugate Chem.* **1999**, *10*, 192–199; c) S. Aime, M. Botta, M. Fasano, G. S. Crich, E. Terreno, *J. Biol. Inorg. Chem.* **1996**, *1*, 312–319.

[9] a) É. Tóth, D. Pubanz, S. Vauthey, L. Helm, A. E. Merbach, *Chem. Eur. J.* **1996**, *2*, 1607–1615; b) L. H. Bryant Jr, M. W. Brechbiel, C. Wu, J. W. M. Bulte, V. Herynek, J. A. Frank, *J. Magn. Reson. Imaging* **1999**, *9*, 348–352; c) G. M. Nicolle, É. Tóth, H. Schmitt-Willich, B. Radüchel, A. E. Merbach, *Chem. Eur. J.* **2002**, *8*, 1040–1048; d) S. Laus, A. Sour, R. Ruloff, É. Tóth, A. E. Merbach, *Chem. Eur. J.* **2005**, *11*, 3064–3076.

[10] a) S. Aime, M. Botta, M. Fasano, S. G. Crich, E. Terreno, *J. Biol. Inorg. Chem.* **1996**, *1*, 312–319; b) P. Caravan, N. J. Cloutier, M. T. Greenfield, S. A. McDermid, S. U. Dunham, J. W. M. Bulte, J. C. Amedio Jr, R. J. Looby, R. M. Supkowski, W. De W. Horrocks Jr, T. J. McMurry, *J. Am. Chem. Soc.* **2002**, *124*, 3152–3162; c) S. Aime, M. Botta, S. G. Crich, G. B. Giovenzana, R. Pagliarin, M. Piccinini, M. Sisti, E. Terreno, *J. Biol. Inorg. Chem.* **1997**, *2*, 470–479.

[11] a) J. P. André, É. Tóth, H. Fisher, A. Seelig, H. R. Mäcke, A. E. Merbach, *Chem. Eur. J.* **1999**, *5*, 2977–2983; b) G. M. Nicolle, É. Tóth, K. P. Eisenwiener, H. R. Mäcke, A. E. Merbach, *J. Biol. Inorg. Chem.* **2002**, *7*, 757–769; c) K. Kimpe, T. N. Parac-Vogt, S. Laurent, C. Piérart, L. Vander Elst, R. N. Muller, K. Binnemans, *Eur. J. Inorg. Chem.* **2003**, *16*, 3021–3027.

[12] a) S. L. Fossheim, A. K. Fahlvik, J. Klaveness, R. N. Muller, *Magn. Reson. Imaging* **1999**, *17*, 83–89; b) V. Weissig, J. Babich, V. Torchilin, *Colloid Surf. B-Biointerfaces* **2000**, *18*, 293–299; c) C. Gløgård, G. Stensrud, R. Hovland, S. L. Fossheim, J. Klaveness, *Int. J. Pharm.* **2002**, *233*, 131–140; d) K.-E. Løkling, S. L. Fossheim, J. Klaveness, R. Skurtveit, *J. Control. Release* **2004**, *98*, 87–95.

[13] a) S. Morel, E. Terreno, E. Ugazio, S. Aime, M. R. Gasco, *Eur. J. Pharm. Biopharm.* **1998**, *45*, 157–163; b) C. Gløgård, G. Stensrud, J. Klaveness, *Int. J. Pharm.* **2003**, *253*, 39–48.

[14] M. Woods, S. Zhang, A. D. Sherry, *Curr. Med. Chem.: Immunol. Endocr. Metab. Agents* **2004**, *4*, 349–369.

[15] S. Laurent, F. Botteman, L. V. Elst, R. N. Muller, *Magn. Reson. Mater. Phys. Biol. Med.* **2004**, *16*, 235–245.

[16] L. V. Elst, F. Maton, S. Laurent, F. Seghi, F. Chapelle, R. N. Muller, *Magn. Reson. Med.* **1997**, *38*, 604–614.

[17] S. Laurent, L. V. Elst, S. Houzé, N. Guérit, R. N. Muller, *Helv. Chim. Acta* **2000**, *83*, 394–406.

[18] R. N. Muller, B. Radüchel, S. Laurent, J. Platzek, C. Piérart, P. Mareski, L. Vander Elst, *Eur. J. Inorg. Chem.* **1999**, 1949–1955.

[19] S. Laurent, F. Botteman, L. V. Elst, R. N. Muller, *Helv. Chim. Acta* **2004**, *87*, 1077–1089.

[20] a) R. Ruloff, É. Tóth, R. Scopelliti, R. Tripier, H. Handel, A. E. Merbach, *Chem. Commun.* **2002**, 2630–2631; b) L. Burai, É. Tóth, A. E. Merbach, *Chem. Commun.* **2003**, 2680–2681; c) S. Laus, R. Ruloff, É. Tóth, A. E. Merbach, *Chem. Eur. J.* **2003**, *9*, 3555–3566.

[21] S. Aime, M. Botta, M. Fasano, M. P. M. Marques, C. F. G. C. Geraldes, D. Pubanz, A. E. Merbach, *Inorg. Chem.* **1997**, *36*, 2059–2068.

[22] a) F. A. Dunand, R. S. Dickins, D. Parker, A. E. Merbach, *Chem. Eur. J.* **2001**, *7*, 5160–5167; b) M. Woods, Z. Kovacs, S. Zhang, A. D. Sherry, *Angew. Chem. Int. Ed.* **2003**, *42*, 5889–5892; c) J. Rudovský, P. Cígler, J. Kotek, P. Hermann, P.

Vojtíšek, I. Lukeš, J. A. Peters, L. V. Elst, R. N. Muller, *Chem. Eur. J.* **2005**, *11*, 2373–2384.

[23] S. Torres, J. A. Martins, J. P. André, C. F. G. C. Geraldes, A. E. Merbach, É. Tóth, *Chem. Eur. J.* **2006**, *12*, 940–948.

[24] J. C. Amedio Jr, P. J. Bernard, M. Fountain, G. V. Wagenen Jr, *Synth. Commun.* **1999**, *29*, 2377–2391.

[25] *IUPAC Stability Constants*, Academic Software, and K. J. Powell, Release 1.05, Yorks, LS21 2PW (UK), **1999**.

[26] Y.-M. Wang, C.-H. Lee, G.-C. Liu, R.-S. Sheu, *J. Chem. Soc. Dalton Trans.* **1998**, 4113–4118.

[27] J. D. Clark, D. Q. Perrin, *Q. Rev.* **1964**, *18*, 295–320.

[28] S. Laurent, L. V. Elst, A. Vroman, R. N. Muller, *Helv. Chim. Acta* **2007**, *90*, 562–573.

[29] G. R. Choppin, *J. Less-Common Met.* **1985**, *112*, 193–205.

[30] J. L. Sudmeier, C. N. Reilley, *Anal. Chem.* **1964**, *36*, 1698–1706.

[31] C. F. G. C. Geraldes, A. M. Urbano, M. C. Alpoim, A. D. Sherry, K. T. Kuan, R. Rajagopalan, F. Maton, R. N. Muller, *Magn. Reson. Imaging* **1995**, *13*, 401–420.

[32] E. N. Rizkalla, G. R. Choppin, W. P. Cacheris, *Inorg. Chem.* **1993**, *32*, 582–586.

[33] J. A. Peters, *Inorg. Chem.* **1988**, *27*, 4686–4691.

[34] B. G. Jenkins, R. B. Lauffer, *J. Magn. Reson.* **1988**, *80*, 328–336.

[35] B. G. Jenkins, R. B. Lauffer, *Inorg. Chem.* **1988**, *27*, 4730–4738.

[36] S. Cortes, E. Brücher, C. F. G. C. Geraldes, A. D. Sherry, *Inorg. Chem.* **1990**, *29*, 5–9.

[37] F. A. Dunand, A. Borel, A. E. Merbach, *J. Am. Chem. Soc.* **2002**, *124*, 710–716.

[38] O. V. Yazyev, L. Helm, *J. Chem. Phys.* **2006**, *125*, 545031-8.

[39] D. H. Powell, O. M. N. Dhubhghaill, D. Pubanz, L. Helm, Y. S. Lebedev, C. Schlaepfer, A. E. Merbach, *J. Am. Chem. Soc.* **1996**, *118*, 9333–9346.

[40] L. Helm, *Prog. NMR Spect.* **2006**, *49*, 45–64.

[41] P. H. Fries, E. Belorizky, *J. Chem. Phys.* **2005**, *123*, 124510-1.

[42] J. Kowalewski, D. Kruk, G. Parigi in *Advances in Inorganic Chemistry* (Eds.: R. Van Eldik, I. Bertini), Elsevier, San Diego, **2005**.

[43] J. Kotek, P. Lebdušková, P. Hermann, L. V. Elst, R. N. Muller, C. F. G. C. Geraldes, T. Maschmeyer, I. Lukeš, J. A. Peters, *Chem. Eur. J.* **2003**, *9*, 5899–5915.

[44] A. Borel, É. Tóth, L. Helm, A. Janóssy, A. E. Merbach, *Phys. Chem. Chem. Phys.* **2000**, *2*, 1311–1317.

[45] L. Burai, É. Tóth, G. Moreau, A. Sour, R. Scopelliti, A. E. Merbach, *Chem. Eur. J.* **2003**, *9*, 1394–1404.

[46] S. Rast, A. Borel, L. Helm, E. Belorizky, P. H. Fries, A. E. Merbach, *J. Am. Chem. Soc.* **2001**, *123*, 2637–2644.

[47] S. Laurent, L. V. Elst, F. Copoix, R. N. Muller, *Invest. Radiol.* **2001**, *36*, 115–122.

[48] H. M. Irving, M. G. Miles, L. Pettit, *Anal. Chim. Acta* **1967**, *38*, 475–488.

[49] L. Zékány, I. Nagypál in *Computational Methods for Determination of Formation Constants* (Ed.: D. J. Leggett), Plenum, N. Y., **1985**, p. 291.

[50] P. K. Glasoe, F. A. Long, *J. Phys. Chem.* **1960**, *64*, 188–190.

[51] G. Brunisholz, M. Randin, *Helv. Chim. Acta* **1959**, *42*, 1927–1938.

[52] A. D. Hugi, L. Helm, A. E. Merbach, *Helv. Chim. Acta* **1985**, *68*, 508–521.

[53] I. Solomon, *Phys. Rev.* **1955**, 559–565.

[54] J. Reuben, *J. Phys. Chem.* **1971**, *75*, 3164–3167.

[55] F. Yerly, *VISUALISEUR 2.3.4*, and *OPTIMISEUR 2.3.4*, Lausanne (Switzerland), **1999**.